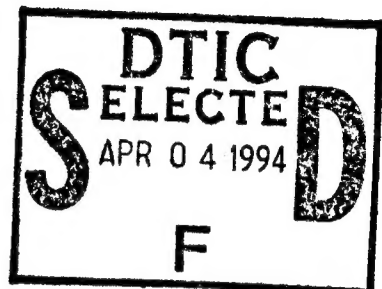


PL-TR-94-2260

SSS-DTR-94-14821

Investigation of Regional Seismic Discrimination Issues for Small or Decoupled Nuclear Explosions

Theron J. Bennett
Brian W. Barker
John R. Murphy



Maxwell Laboratories, Incorporated
S-CUBED Division
P. O. Box 1620
La Jolla, CA 92038-1620

October, 1994

Scientific Report No. 1

19950403 021

Approved for Public Release; Distribution Unlimited



PHILLIPS LABORATORY
Directorate of Geophysics
AIR FORCE MATERIEL COMMAND
HANSCOM AIR FORCE BASE, MA 01731-3010

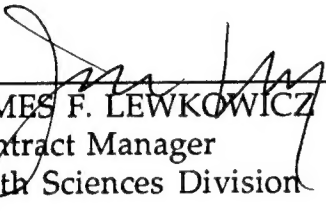
DTIC QUALITY INSPECTED 1

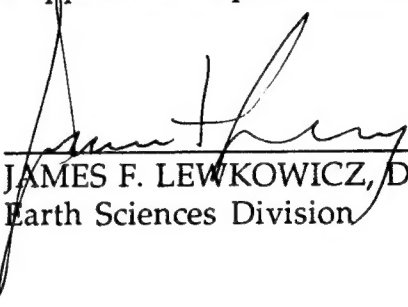
SPONSORED BY
Advanced Research Projects Agency (DoD)
Nuclear Monitoring Research Office
ARPA ORDER NO A128

MONITORED BY
Phillips Laboratory
CONTRACT NO. F19628-93-C-0093

The views and conclusions contained in this document are those of the authors and should not be interpreted as representing the official policies, either express or implied, of the Air Force or the U.S. Government.

This technical report has been reviewed and is approved for publication.


JAMES F. LEWKOWICZ
Contract Manager
Earth Sciences Division


JAMES F. LEWKOWICZ, Director
Earth Sciences Division

This report has been reviewed by the ESC Public Affairs Office (PA) and is releasable to the National Technical Information Service (NTIS).

Qualified requestors may obtain additional copies from the Defense Technical Information Center. All others should apply to the National Technical Information Service.

If your address has changed, or if you wish to be removed from the mailing list, or if the addressee is no longer employed by your organization, please notify PL/TSI, 29 Randolph Road, Hanscom AFB, MA 01731-3010. This will assist us in maintaining a current mailing list.

Do not return copies of this report unless contractual obligations or notices on a specific document requires that it be returned.

REPORT DOCUMENTATION PAGE			Form Approved OMB No. 0704-0188
<p>Public reporting burden for this collection of information is estimated to average 1 hour per response, including the time for reviewing instructions, searching existing data sources, gathering and maintaining the data needed, and completing and reviewing the collection of information. Send comments regarding this burden estimate or any other aspect of this collection of information, including suggestions for reducing this burden, to Washington Headquarters Services, Directorate for Information Operations and Reports, 1215 Jefferson Davis Highway, Suite 1204, Arlington, VA 22202-4302, and to the Office of Management and Budget, Paperwork Reduction Project (0704-0188), Washington, DC 20503.</p>			
1. AGENCY USE ONLY (Leave blank)	2. REPORT DATE	3. REPORT TYPE AND DATES COVERED	
	October, 1994	Scientific No. 1	
4. TITLE AND SUBTITLE		5. FUNDING NUMBERS	
Investigation of Regional Seismic Discrimination Issues for Small or Decoupled Nuclear Explosions		Contract #: F19628-93-C-0093 PE 62301E PR NM93 TA GM WU AF	
6. AUTHOR(S)		8. PERFORMING ORGANIZATION REPORT NUMBER	
Theron J. Bennett, Brian W. Barker, and John R. Murphy		SSS-DTR-94-14821	
7. PERFORMING ORGANIZATION NAME(S) AND ADDRESS(ES)		9. SPONSORING/MONITORING AGENCY NAME(S) AND ADDRESS(ES)	
Maxwell Laboratories, Inc. S-CUBED Division P.O. Box 1620 La Jolla, CA 92038-1620		Phillips Laboratory 29 Randolph Road Hanscom AFB, MA 01731-3010 Contract Manager: James F. Lewkowicz/GPEH	
10. SPONSORING/MONITORING AGENCY REPORT NUMBER		11. SUPPLEMENTARY NOTES	
PL-TR-94-2260			
12a. DISTRIBUTION/AVAILABILITY STATEMENT		12b. DISTRIBUTION CODE	
Approved for public release; distribution unlimited			
13. ABSTRACT (Maximum 200 words)			
<p>The goals of lowering the seismic threshold for underground nuclear explosions to magnitudes near 2.5 m_b and extending the capability to other geographical regions will require utilization of regional stations for detection and identification. However, regional techniques have seldom been tested on small nuclear explosions. Therefore, S-CUBED is conducting a research program aimed at the identification problems associated with small or decoupled nuclear explosions near a low monitoring threshold (e.g. 1-kt fully decoupled or about 2.5 m_b). Initial efforts have focused on using source scaling procedures to scale down records from larger explosions and produce representative seismograms at ARPA regional array stations. The scaled signals embedded in typical background noise at the station enable an assessment of capabilities for different regional signal analysis methods at the lower thresholds. Our preliminary findings are that useful far-regional signals from small or decoupled nuclear explosions may be constrained to very limited high-frequency bands, which may limit the capabilities of some regional detection and identification techniques.</p>			
14. SUBJECT TERMS			15. NUMBER OF PAGES
Seismic Discrimination Scandinavia			50
Explosion Regional			16. PRICE CODE
17. SECURITY CLASSIFICATION OF REPORT	18. SECURITY CLASSIFICATION OF THIS PAGE	19. SECURITY CLASSIFICATION OF ABSTRACT	20. LIMITATION OF ABSTRACT
UNCLASSIFIED	UNCLASSIFIED	UNCLASSIFIED	UNLIMITED

Table of Contents

	<u>Page</u>
1. Introduction.....	1
2. Review of Source Scaling Theory.....	4
2.1 Seismic Source Scaling Theory.....	4
2.2 Magnitude, Yield, and Elastic Radius Relationships.....	8
2.3 Influence of Decoupling.....	10
3. Explosion Database and Noise Samples.....	12
4. Application of Scaling Theory to Regional Array Data.....	17
4.1 Procedures and Results.....	17
4.2 Comparison to Prior Studies.....	27
4.3 Comparison to the December 31, 1992 NZ Event.....	32
5. Summary and Conclusions.....	36
6. References.....	38

List of Illustrations

	<u>Page</u>
1 Predicted decoupling factor as a function of frequency based on source scaling theory relating a 1-kt tamped nuclear explosion to a 1-kt fully-decoupled nuclear explosion.....	11
2 Locations of nuclear explosion sources and ARPA regional array stations.....	13
3 Source scaling factor as a function of frequency for explosions of different yields characterized by their elastic radii (r_1) relative to a larger explosion with an elastic radius of 685 m (r_2).....	19
4 Examples of application of source-scaling process to NZ explosion at ARPA regional arrays.....	21
5 Examples of application of source-scaling process to PNE explosion at NORESS.....	23
6 Comparison of regional P-wave Fourier spectra determined from ARA0 record of 10/24/90 NZ explosion before and after scaling to 1-kt decoupled relative to spectrum of background noise.....	25
7 Comparison of regional S-wave Fourier spectra determined from ARA0 record of 10/24/90 NZ explosion before and after scaling to 1-kt decoupled relative to spectrum of background noise.....	26
8 Extended broadband waveform segments for selected ARCESS elements simulating a 1-kt decoupled nuclear explosion from NZ embedded in typical background noise.....	28
9 Bandpass filtered (6 - 12 Hz) waveform segments for the same channels for the simulation of a 1-kt decoupled nuclear explosion from NZ in typical background noise.....	29

10	Variations in monitoring thresholds from Novaya Zemlya (excluding time intervals of observed events) for the NORESS and ARCESS regional arrays during the month of February, 1992 (adapted from Kvaerna, 1992).....	31
11	Application of band-pass filter analysis to vertical component ARA0 recording of the 12/31/92 unknown event at Novaya Zemlya.....	34
12	Application of band-pass filter analysis to vertical component ARA0 recording of the 10/24/90 NZ explosion scaled down to 1-kt fully decoupled.....	35

List of Tables

	<u>Page</u>
1 Explosion Database and Noise Samples.....	14
2 Yield Relationships.....	18

Accesion For	
NTIS	CRA&I <input checked="" type="checkbox"/>
DTIC	TAB <input type="checkbox"/>
Uriannounced <input type="checkbox"/>	
Justification	
By	
Distribution /	
Availability Codes	
Dist	Avail and / or Special
A-1	

1. Introduction

Seismic techniques have long provided a primary tool for monitoring underground nuclear weapons testing. Teleseismic monitoring generally has proven to be adequate for detection and identification of underground nuclear explosion tests down to magnitude levels near 4.0 mb in areas of interest, such as the former Soviet Union (cf. OTA, 1988). However, the goals of lowering the threshold to magnitudes near 2.5 mb and extending the capability to other geographical regions will require significant improvements in monitoring capability. These objectives require the utilization of regional stations for detection and identification. Unfortunately, these goals have proven to be elusive because of the complexity of regional seismic signals, their dependence on propagation effects, and incomplete theoretical understanding of source influences on regional signal generation. Nevertheless, several regional seismic identification techniques have been investigated and found to be useful in discriminating underground nuclear explosions from earthquakes for some source/propagation environments.

The capability for regional seismic monitoring in several areas of Eurasia has improved significantly in recent years with the advent of the high-quality ARPA regional arrays at NORESS, ARCESS, GERESS, and FINESA. These arrays are now routinely providing excellent regional seismic data for events in Scandinavia and northern Europe, and additional development of regional arrays in other parts of Eurasia is enhancing regional monitoring in those areas. A limitation on testing regional discrimination methods with the data from these new arrays is that the available database does not include many nuclear explosions. Furthermore, the nuclear explosions which have been recorded by these arrays generally have been large and cannot be used directly to test the IMS/NMRD monitoring system at low thresholds. Most discrimination studies with these regional arrays, therefore, have had to rely on comparisons between the signals from mineblasts, small earthquakes, and mining-induced events. Extrapolation of regional discrimination results based on these alternate source types cannot be regarded as

definitive for identifying potential small or decoupled underground nuclear explosion tests.

Therefore, S-CUBED is conducting a research program aimed at the identification problems associated with small or decoupled nuclear explosions near a low monitoring threshold (e.g. 1-kt decoupled, approximately 2.5 mb). Our initial efforts in this area have focused on using Mueller-Murphy source scaling to produce representative seismograms at regional array stations for these low-threshold nuclear explosions. To test the methodology and to provide a relatively clean example, we have used the source-scaling theory to modify the available records at the ARPA regional arrays in Scandinavia from several nuclear explosions in the former Soviet Union at far-regional epicentral distances. The scaled signals embedded in records typical of background noise at the station enable an assessment of the detection and identification capabilities of different regional signal analysis methods at the lower thresholds. In particular, the modified signals at the regional arrays will be processed by the IMS/NMRD system to give more realistic assessments of monitoring capabilities and limitations at low thresholds.

The source scaling procedures were applied to the signals recorded at NORESS, ARCESS, and FINESA regional arrays from three nuclear explosions including two NZ events and one PNE north of Arkhangel'sk. The records were scaled down to 1-kt fully decoupled producing a reduction in amplitude and frequency shift toward higher frequencies. The scaled signals were superimposed on a variety of noise samples from the same stations including several long signal-free waveform segments. Our preliminary findings are that the signals were usually difficult to discern on the broadband records. The useful far-regional signals from small or decoupled nuclear explosions may be constrained to very limited high-frequency bands. This may limit the capabilities of some regional detection and identification techniques. A digital tape containing the results of the initial scaling studies for two different noise segments has been supplied to the ARPA Center for Seismic Studies for further processing and testing of the IMS/NMRD system.

This report describes the results of the initial phases of this research. The report is divided into five sections including these introductory comments. Section 2 summarizes the source scaling theory which has been used to scale the explosion records to lower yields. Section 3 describes the data used for scaling and the background noise. The application of the source scaling theory to the far-regional waveform data and characteristics of the resulting signals in relation to the ambient seismic noise are presented in Section 4. Finally, Section 5 presents some preliminary observations and plans for further work.

2. Review of Source Scaling Theory

Small underground nuclear explosion tests have seldom been well recorded at epicentral distances in the regional to far-regional range. This is partly the result of the lack of high-quality regional stations at quiet sites with sufficient dynamic range to record such events. With the high monitoring thresholds governed by treaties, there has been limited practical interest in identifying small events. Except for the western U.S., little knowledge has been available of the actual occurrence of small nuclear explosions. Even there the regional signals from small events have not always been well recorded because of high attenuation related to geologic structure and tectonic complexity. Therefore, actual regional seismic data is inadequate for testing the monitoring system for small or decoupled nuclear explosion tests in most regions of the world. However, it may be possible to obtain reasonable simulations of the regional seismic signals from these kinds of small events by applying source scaling theory to the signals from well-recorded larger events.

2.1 Seismic Source Scaling Theory

According to source scaling theory, if we let $Z_1(t)$ and $Z_2(t)$ represent the seismogram time histories for a particular component of the ground motion recorded at the same station from two different explosions at the same source location, then the corresponding ground motion spectra, $Z_1(\omega)$ and $Z_2(\omega)$ can be written as

$$\begin{aligned} Z_1(\omega) &= S_1(\omega) T(\omega) \\ Z_2(\omega) &= S_2(\omega) T(\omega) \end{aligned} \tag{1}$$

where $S_1(\omega)$ and $S_2(\omega)$ are the seismic source spectra for the two explosions and $T(\omega)$ is the propagation path transfer function common to the two events. We can then express the ground motion spectrum for one explosion in terms of the spectrum for the other as

$$Z_2(\omega) = \frac{S_2(\omega)}{S_1(\omega)} Z_1(\omega)$$

So, if we can estimate the seismic source functions for the two explosions, we can predict the ground motion spectrum for the second explosion based on the observed spectrum for the first explosion.

The seismic source function for underground nuclear explosions accounts for the coupling of energy released by the explosion into the seismic wave field radiated outward from the source. Rodean (1981) and Bache (1982) reviewed much of the early work aimed at developing quantitative understanding of seismic coupling and the seismic source function for explosion sources. The ground motion is usually developed in terms of a reduced displacement potential which depends on the material properties of the source region, depth, and explosion yield. Theoretical models based on constitutive behavior of the near source geologic materials can be used to determine the potential function. However, in this discussion we follow the development of Mueller and Murphy (1971) or von Seggern and Blandford (1972) which present the reduced displacement potential as an analytic function which is constrained by empirical observations from prior underground nuclear explosions.

For a simple, spherically symmetric model of the explosion source, the displacement spectrum (cf. Mueller and Murphy, 1971) can be represented as

$$Z(\omega) = \left(\frac{p(\omega) r_{el}}{4\mu} \right) \left(\frac{1}{r^2} + \frac{i\omega}{r\alpha} \right) \frac{\alpha^2}{(\omega_0^2 + i\omega_0\omega - \beta\omega^2)} \quad (2)$$

where $p(\omega)$ is the Fourier transform of the spherically symmetric pressure from the explosion acting at the elastic radius, r_{el} , and

$$\omega_0 = \frac{\alpha}{r_{el}}$$

$$\beta = \frac{\lambda + 2\mu}{4\mu}$$

where α is the compressional wave velocity and λ and μ are the Lame constants characteristic of the source medium. Using this relation the source spectral ratio for the two explosions is then

$$\frac{S_2(\omega)}{S_1(\omega)} = \frac{p_2(\omega)}{p_1(\omega)} \frac{r_{el_2}}{r_{el_1}} \frac{\omega_{01}^2 + i\omega_{01}\omega - \beta\omega^2}{\omega_{02}^2 + i\omega_{02}\omega - \beta\omega^2}$$

For explosions at the same depth in a fixed medium, the elastic transition pressure should be constant; then, assuming a step-function approximation for the pressure profiles acting at the elastic radii, it follows that $p_2(\omega) = p_1(\omega)$ and that the modulus of the source spectral ratio can be written simply as

$$|S(\omega)| = \frac{|S_2(\omega)|}{|S_1(\omega)|} = \frac{r_{el_2}}{r_{el_1}} \sqrt{\frac{(\omega_{01}^2 - \beta\omega^2)^2 + \omega_{01}^2\omega^2}{(\omega_{02}^2 - \beta\omega^2)^2 + \omega_{02}^2\omega^2}} \quad (3)$$

From this it can be seen that the low- and high-frequency asymptotic values of the source spectral ratio are given by

$$\lim_{\omega \rightarrow 0} |S(\omega)| = \left(\frac{r_{el_2}}{r_{el_1}} \right)^3 \quad (4)$$

$$\lim_{\omega \rightarrow \infty} |S(\omega)| = \frac{r_{el_2}}{r_{el_1}}$$

or, since r_{el} is proportional to the cube root of the yield, Y , for explosions at the same depth of burial in a given source medium,

$$\lim_{\omega \rightarrow 0} |S(\omega)| = \frac{Y_2}{Y_1}$$

$$\lim_{\omega \rightarrow \infty} |S(\omega)| = \left(\frac{Y_2}{Y_1} \right)^{\frac{1}{3}}$$

Thus, at low frequencies the ratio of the source spectra of the two explosions is just equal to the ratio of their yields; while at the high frequency limit the ratio of the source spectra is equal to the cube root of the yield ratio.

With some simplifications the seismogram in the time domain from one explosion can be expressed in terms of the seismogram from another explosion with different source characteristics but in the same region as follows

$$Z_2(t) = \int_{-\infty}^{\infty} Z_1(\tau) S_1(t - \tau) d\tau + \frac{r_{el_2}}{r_{el_1}} Z_1(t) \quad (5)$$

where

$$S_1(t) = -\frac{r_{el_2}}{r_{el_1}} e^{-\frac{2}{3}\omega_{02}t} \left[C_1 \cos \frac{2\sqrt{2}}{3} \omega_{02} t + C_2 \sin \frac{2\sqrt{2}}{3} \omega_{02} t \right]$$

with

$$C_1 = \frac{4}{3}(\omega_{02} - \omega_{01})$$

and

$$C_2 = \frac{\sqrt{2}}{3}\omega_{02} \left[1 + 2\frac{\omega_{01}}{\omega_{02}} - 3\left(\frac{\omega_{01}}{\omega_{02}}\right)^2 \right]$$

In the following we have used these scaling relationships to scale down the signals from several large-yield underground nuclear explosions to obtain signals representative of the much smaller yields (approaching 1-kt decoupled) which would be appropriate to the low-threshold monitoring problem.

2.2 Magnitude, Yield, and Elastic Radius Relationships

The scaling relations described above are presented in terms of the elastic radius, the distance from the center of the explosion source beyond which the medium response to the induced motion is approximately linear. The elastic radii for underground nuclear explosions are rarely observed directly. The elastic radii are determined instead indirectly from empirical measurements (e.g. free-field ground motions) and assuming modified cube-root scaling with yield of the form

$$r_{el} = \frac{D Y^{\frac{1}{3}}}{h^{\delta}} \quad (6)$$

where h is source depth and D and δ are constants dependent on material properties of the medium, which are determined empirically. Murphy (1977) showed that near-regional and regional broad-band seismic data and teleseismic body-wave magnitudes are generally consistent with this modified source model for United States explosions in various materials.

In the analyses below we are interested in assessing the influence of the explosion yield difference on the detectability and

identification capability for small nuclear explosions. For this purpose we have assumed a fixed depth of about 150 m for the explosion sources; the influence of alternative assumptions about this fixed source depth will be investigated in future work. For this case at a fixed depth, the scaling law for the elastic radius simplifies to

$$r_{el} = D' Y^{\frac{1}{3}} \quad (7)$$

where, for example, $D' = 186 \text{ m}/\text{kt}^{\frac{1}{3}}$ for explosions in a saturated tuff/rhyolite medium at 150 m source depth.

The above relationship combined with the source scaling theory would be sufficient to perform the desired scaling for explosions of known yield. However, except for some recently published yields of nuclear explosions from the former Soviet Union (cf. Vergino, 1989a,b), we only know the yields for United States nuclear tests. A number of recent studies (e.g. Ringdal et al., 1992) indicate that reasonably accurate estimates of the yields of nuclear explosions at several test areas in the former Soviet Union can be obtained from magnitude-yield relationships.

The magnitude most often used in explosion yield estimation is the teleseismic body-wave magnitude, m_b . The relationship between m_b and yield for application at the Balapan test site has been determined to be

$$m_b = 4.45 + 0.75 \log Y \quad (8)$$

The recently released yields for nuclear explosions in the former Soviet Union confirm that this magnitude-yield relationship probably provides reasonable estimates of the yields for most historic events. For purposes of this study we assume that this same magnitude-yield relationship can be extrapolated to lower magnitude explosions in order to estimate the corresponding yields and is also applicable to

Russian tests in other areas (viz Novaya Zemlya and north of Arkhangel'sk).

2.3 Influence of Decoupling

The final element to be considered in our processing scheme is decoupling. Original theoretical studies predicted that large decoupling factors (> 200) could be achieved for underground nuclear explosions detonated in a cavity. However, subsequent observations have suggested that the maximum achievable decoupling is somewhat lower. As a result of these findings, the current belief is that a decoupling factor of about 70 can be attained at low frequencies (OTA, 1988). A decoupling factor of 70 implies that the low-frequency spectral level for seismic signals from a fully-decoupled explosion would be only about $\frac{1}{70}$ that of a fully-coupled (tamped) explosion of the same yield.

We can consider the influence of this decoupling factor in relation to the explosion source scaling theory presented above. In particular, the scaling relations indicate that the low-frequency spectral ratio behaves as the ratio of the yields while the high-frequency spectral ratio behaves as the cube-root of the ratio of the yields. This implies that the decoupling factor for cavity decoupling of underground explosions is greatly reduced at high frequencies. In particular, if the decoupling factor at low frequencies is taken to be 70, the decoupling factor at high frequencies would be expected to be only about $\sqrt[3]{70}$, or about four to five. At intermediate frequencies the decoupling factor goes through a transition from high to low; the corner frequencies at which the transition occurs are predictable from the scaling theory and are proportional to the ratio of the medium velocity to the elastic radii of the two explosions.

Figure 1 shows the scaling factor relating a 1-kt tamped explosion in granite to a 1-kt fully-decoupled explosion in the same medium. The decoupling factor is about 70 at low frequencies up to about 2 - 3 Hz and drops off to the predicted factor of between 5 and 6 near the 20 Hz upper limit of the plot. Over the intervening frequency range a rapid decrease in the scaling factor is predicted.

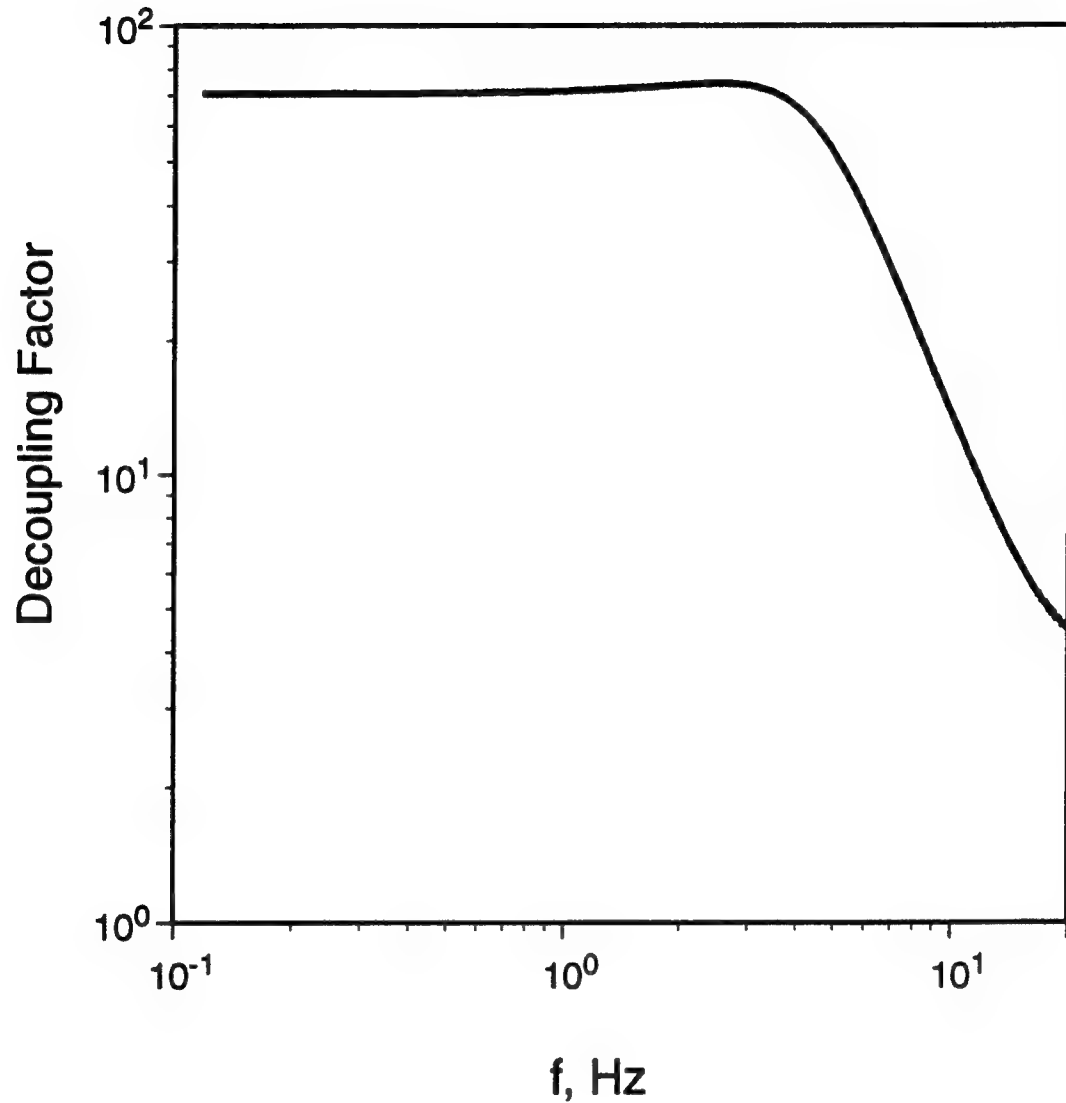


Figure 1. Predicted decoupling factor as a function of frequency based on source scaling theory relating a 1kt tamped nuclear explosion to a 1kt fully-decoupled nuclear explosion.

3. Explosion Database and Noise Samples

As noted above, the database of underground nuclear explosions recorded by the high-quality ARPA regional arrays is extremely sparse. The principal reason for the limited availability of data is that not many nuclear explosion tests have been conducted since the arrays became operational in the late 1980's or early 1990's. In addition, the locations of the arrays in Scandinavia and northern Europe placed them outside the regional distance range of the explosion test sites at Balapan in the former Soviet Union and NTS. As a result, the only regional nuclear explosion seismic data from the ARPA array stations which are available are from more recent Novaya Zemlya (NZ) explosions and a recent PNE test north of Arkhangel'sk and east of the White Sea. We have attempted to recover waveform data from all the regional array stations for all such events which occurred since the first ARPA array became operational at NORESS.

Figure 2 shows the locations of the ARPA regional arrays at NORESS, ARCESS, and FINESA which have been used in these analyses. The map also shows the location of the Novaya Zemlya test site which has been the site of four underground nuclear explosions since 1987 and the location of a single PNE test north of Arkhangel'sk in 1985. Table 1 provides more information about the events and the availability of data at the array stations. The NZ events fall in a very limited magnitude range from 5.6 to 5.8 mb, and the PNE had a magnitude of 5.0 mb. Station availability is generally indicative of the time when the individual arrays became operational. As a result only the most recent (10/24/90) explosion at NZ was recorded by all three regional arrays, and of the ARPA arrays only NORESS recorded the 7/18/85 PNE. The stations generally lie at far -regional distances from the explosion sources. Although locations vary somewhat between events, the epicentral distances from NZ explosions are approximately 2260 km to NORESS, 1100 km to ARCESS, and 1770 km to FINESA. The epicentral distance from the 1985 PNE to NORESS is 1560 km.

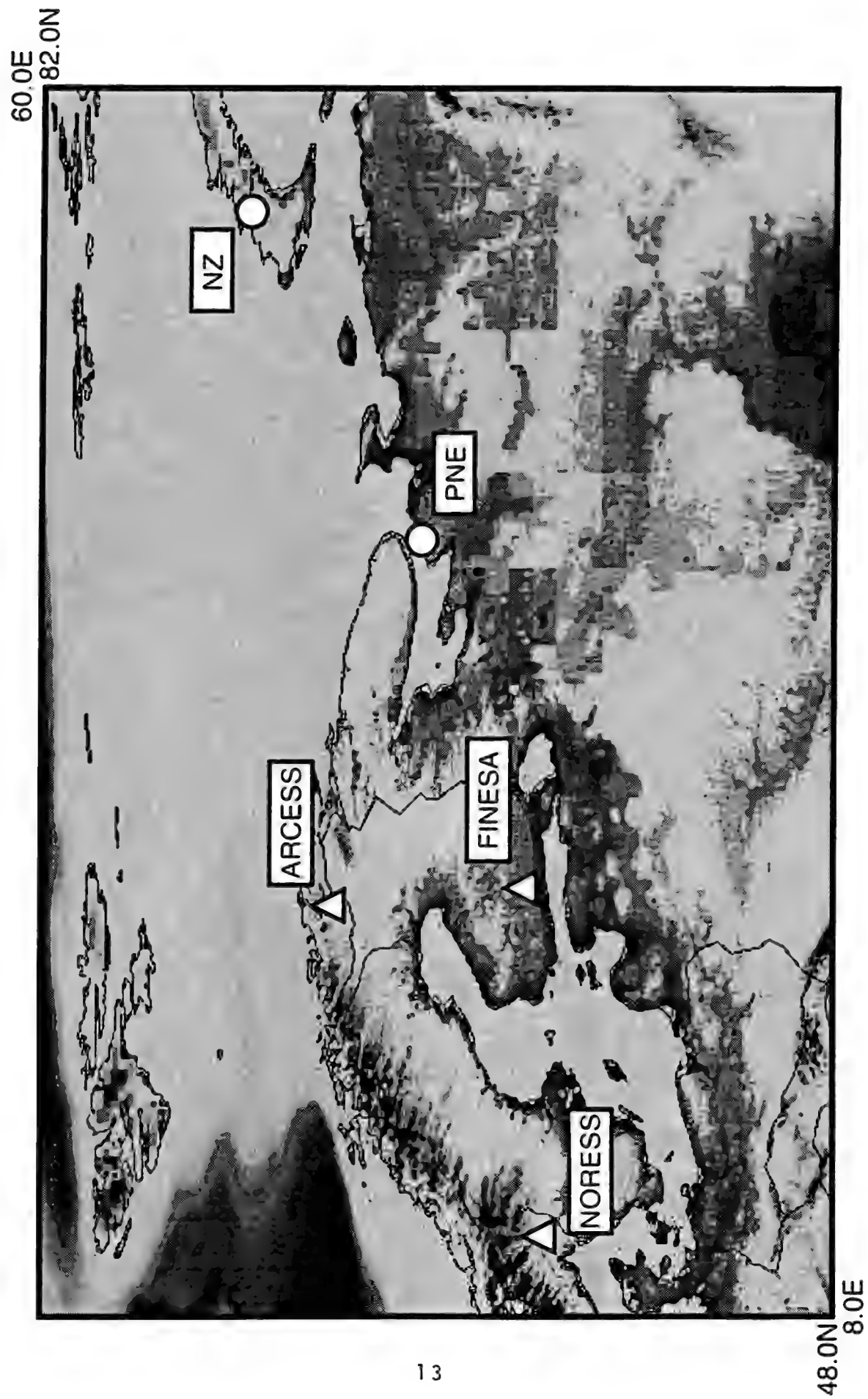


Figure 2. Locations of nuclear explosion sources and ARPA regional array stations.

Table 1
Explosion Database

Date	Origin Time	Lat('N)	Lon('E)	mb	Array Stations
08/02/87	02:00:00	73.34	54.63	5.8	NORESS
05/07/88	22:49:58	73.36	54.45	5.6	NORESS, ARCESS
12/04/88	05:19:53	73.39	55.00	5.7	NORESS, ARCESS
10/24/90	14:57:58	73.36	54.71	5.7	NORESS, ARCESS, FINESA
07/18/85	21:14:57	65.97	40.86	5.0	NORESS

Noise Samples

Date	Time	Duration (sec)	Array Stations
04/23/92	05:15:00	1500	NORESS, ARCESS, FINESA
06/28/92	12:30:00	1500	NORESS, ARCESS
06/28/92	15:37:00	1500	NORESS, FINESA

The waveform segments used in these analyses were recovered from the IMS database at the Center for Seismic Studies (CSS). For each event we obtained the entire waveform segments which were available around the predicted signal arrival times at each station for all array elements. The data quality was generally good except for a few spikes and data dropouts. These problem data segments were either not used or corrected by substitution of a similar segment. In all cases the waveform segments extend from prior to P through the Lg group velocity window. The recorded signals are generally strong with complex regional P, S, and Lg. Broadband signal-to-noise ratios (S/N) are quite variable between events, stations, and array elements. In general, S/N for the NZ events is much greater than 100 at NORESS and ARCESS but less than about 50 at FINESA. The broadband S/N at NORESS for the PNE event is somewhat smaller (between 50 and 100).

The characteristics of the far-regional signals at the ARPA array stations will be described in more detail in the following report section. For the broadband records the P signals show a sharp onset at all three arrays. The P signals in all cases appear quite complex with apparent multiple regional arrivals. At the nearest station, ARCESS, the complex P and regional S signals have roughly comparable maximum amplitudes on the broadband recordings for the NZ explosions. At FINESA the broadband regional P signals are approximately twice as large as the maximum amplitude in the dispersed Lg window. At NORESS the maximum amplitude in the P window is at least four-to-five times as large as the maximum amplitude in the Lg window for the NZ events but only about twice as large for the PNE event. In addition, the NORESS recordings for the PNE appear to show some distinction between the regional S coda and a later-arriving Lg phase possibly due to greater dispersion over this path.

In our analysis procedure we also require waveform segments representative of the background noise at each of the array stations. Our search for long noise segments from the IMS database at CSS produced only limited success. Most of the waveform data currently available there from the ARPA arrays corresponds to detected signals

or events. With some effort three relatively long record segments with no apparent signals were identified. These are described at the bottom of Table 1. The selected noise segments were approximately 25 minutes in duration. Subsequent band-pass filtering of the segments revealed possible signals or above normal noise conditions at high frequencies near the ends of some segments, and we were forced to truncate those time histories for use in the applications which followed.

The broadband characteristics of the noise segments in Table 1 appear to be typical of those observed at the ARPA array stations. In particular, the lowest noise based on the maximum broadband amplitudes from these segments appears to be that at NORESS; the noise at ARCESS is more than twice as large; and the FINESA noise is midway between the other two. The maximum noise amplitudes vary by up to 30 percent between station elements at individual arrays for these segments. Studies by Kvaerna and Ringdal (1991) suggest that larger variations in background noise levels may be expected dependent on the time of year and time of day. In future work we plan to investigate the influences of such noise variations in greater detail. As noted above, the long noise segments which we have used here were available for only two dates and do not show great differences. We have also compared the noise behavior in these long segments with that from the pre-P noise segments for the explosion records from Table 1. In general, the broadband peak noise amplitudes from these segments are in the same range as those from the long noise segments. The records from the 5/07/88 NZ explosion appear to be exceptional in that the pre-P noise is only about half as large as that for the other records in Table 1. Reasons for this discrepancy are unknown, but these records have other problems with data dropouts and have not been used in any of the subsequent applications.

4. Application of Scaling Theory to Regional Array Data

The source scaling theory described in Section 2 of this report has been applied to the database described in Section 3. Our objective was to scale down the signals from the large NZ and PNE explosions recorded at the ARPA regional arrays to the low thresholds (e.g. 1-kt decoupled) which are being discussed in conjunction with more comprehensive test ban treaties. Our initial focus has been on three events: the 12/04/88 and 10/24/90 NZ explosions and the 7/18/85 PNE. We have assessed the detectability of the scaled regional signals from these events in relation to the noise segments described in the preceding section and have generated complete array data segments for the scaled signals embedded in extended versions of the noise samples. The simulated time histories can be used to test the IMS system and regional discrimination capabilities for low-yield and decoupled nuclear explosion tests.

4.1 Procedures and Results

The 12/04/88 and 10/24/90 NZ explosions had similar magnitudes of 5.7 mb as shown in Table 1 above. To utilize the explosion source scaling, we need to have the equivalent elastic radius. Table 2 summarizes the magnitude-yield-elastic radius relations relevant to this application. Assuming the NZ explosions were fully tamped, we see that 5.7 mb corresponds to a yield of about 50 kt and an elastic radius of 685 m. We further see that an explosion of 1-kt fully decoupled has an equivalent elastic radius of 45 m and would be expected to produce a magnitude of 2.6 mb.

Figure 3 shows the theoretical source scaling factors as a function of frequency for four explosion source models with different yields relative to the large explosion with elastic radius of 685 m (50-kt tamped). As can be seen by comparing with Table 2, the scaling factors shown correspond to 1-kt fully tamped ($r_{el} = 186$ m), 10-kt fully decoupled ($r_{el} = 97$ m), 5-kt fully decoupled ($r_{el} = 77$ m), and 1-kt fully decoupled ($r_{el} = 45$ m). The theory predicts significant reductions in

Table 2
Yield Relationships

$$m_b = 4.45 + 0.75 \log Y \text{ (Fully Tamped)}$$

$$m_b = 2.60 + 0.75 \log Y \text{ (Fully Decoupled)}$$

$$r_{el} = 186 Y^{\frac{1}{3}}$$

<u>Fully Tamped</u>			<u>Fully Decoupled</u>		
m_b	Yield (kt)	r_{el} (m)	m_b	Yield (kt)	r_{el} (m)
6.08	150	988	4.23	150	240
5.95	100	863	4.10	100	209
5.72	50	685	3.87	50	166
5.20	10	401	3.35	10	97
4.97	5	318	3.12	5	77
4.45	1	186	2.60	1	45

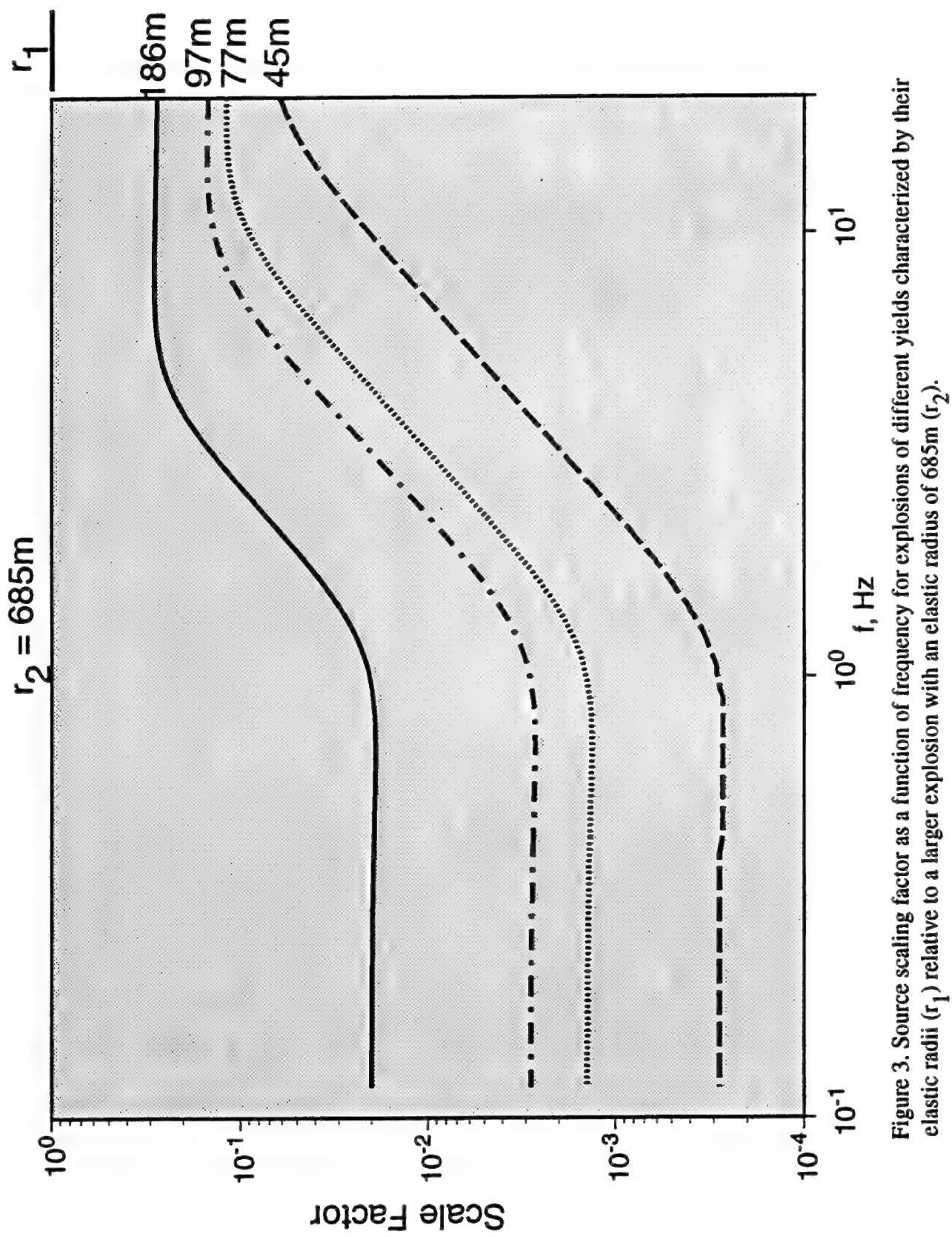


Figure 3. Source scaling factor as a function of frequency for explosions of different yields characterized by their elastic radii (r_1) relative to a larger explosion with an elastic radius of 685m (r_2).

amplitude for the smaller events. The amplitude reductions are predicted to be much larger at low frequencies (1 Hz and below) than at high frequencies. Comparing low-frequency levels for 1-kt fully tamped ($r_{el} = 186$ m) and 1-kt fully decoupled ($r_{el} = 45$ m), we note that the scaling factors are different by a factor of 70 which is just the maximum decoupling factor achievable according to empirical results.

Focusing on the scale factor for the 45 m elastic radius (1-kt fully decoupled) relative to the 685 m elastic radius (50-kt tamped), we see that source scaling theory predicts a reduction in amplitude of 3500 at low frequencies. At high frequencies (approaching 20 Hz) the predicted amplitude reduction is only about 15 (i.e. $\sqrt[3]{3500}$). Over the interval from 1 Hz to 20 Hz, the scale factor shows a very gradual increase. Application of this scale factor to the Fourier spectrum of the original seismogram would be expected to produce a pronounced shift in frequency content. The final step in the procedure is then to add the scaled seismogram signals into the noise segments.

Figure 4 illustrates the application of the scaling process to the 12/24/90 NZ explosion. Similar results were obtained for the 12/04/88 explosion and the alternative noise sample. In the original broadband records at the top of the figure, we see the large amplitude regional signals with sharp P onsets at all three array stations. The P signal shows some complexity with the coda gradually decreasing before the arrival of complex regional S and Lg phases. The regional S/Lg phase has a relatively clear onset at ARA0 but not at FIA0 or NRA0 where the signal level is relatively low and dispersed in character.

The next set of three records shows the effect of scaling on the same signals at the three stations. The reduction in the peak amplitude is about a factor of 200 at ARA0 and between 400 and 500 at NRA0. However, at FIA0 the peak amplitude appears to be reduced by only about a factor of 70. FIA0 appears somewhat anomalous too because of the apparent spike later in the regional P signal. We are continuing to investigate this anomaly. Our preliminary interpretation is that the high-frequency spike is an aberration caused by a brief interval of clipping on the FINESA records for the original NZ explosion. Looking at the signals away from the spike time, maximum amplitudes on the scaled trace are

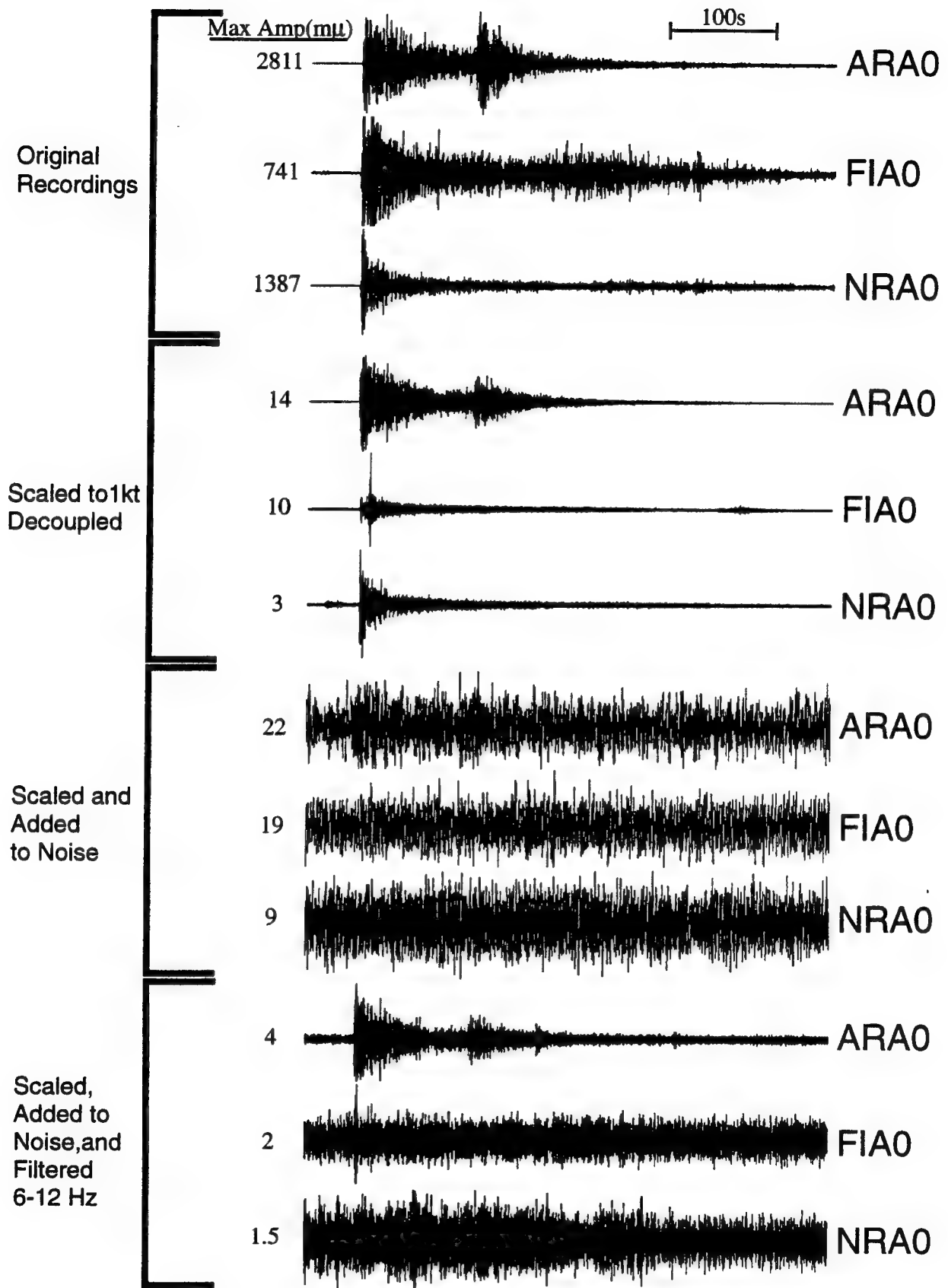


Figure 4. Examples of application of source-scaling process to NZ explosion at ARPA regional arrays.

about a factor of three lower, or about $3 \text{ m}\mu$. The original (unscaled) FIA0 trace appears to be only moderately clipped, so that the maximum amplitude is probably not much greater than $750 \text{ m}\mu$. Accepting these revised values and ignoring the spikes, the effect of scaling on the signals at FIA0 appears to reduce the maximum amplitude by about a factor of 250. The scaling procedure also seems to reduce the significance of later regional phases relative to the original P. This might be associated with relatively greater high-frequency content in the regional P compared to other regional phases which is enhanced in the scaling process.

The third set of three records shows the broadband scaled records added into the 04/23/92 noise segments. In all cases the noise level on the broadband records is greater than the scaled signal records. There may still be some indication of the P signal at ARA0 associated with a frequency shift and moderate amplitude increase at about the expected P arrival time. However, the results suggest that the broadband records would not be particularly useful for detecting or measuring the strength of regional signals from such small explosions in this far-regional distance range.

Finally, the bottom three records show the results of application of a bandpass filter to the scaled records superimposed on the noise. We applied a series of several different filters to the time histories. In general, no signals could be seen in the low-frequency bands (below about 3 Hz) at any of the stations. However, the higher frequency passbands did show signals at some stations. In particular, we see here regional P, S and Lg in the 6 - 12 Hz frequency band at ARA0. There is also a possible arrival at FIA0 near the expected P time which rises above the noise in this same 6 - 12 Hz band; but we discount this detection because it appears likely that it is associated with the clipping problem at FINESA cited above.

Figure 5 shows the same process applied to the NRA0 record at a range of about 1560 km for the 7/18/85 PNE. In this case the original explosion had a magnitude of 5.0 mb corresponding to a yield of about 5 kt tamped. We again have scaled the signal down to 1-kt decoupled using the source scaling theory. The original broadband time history at the top shows large signals with clear indications of

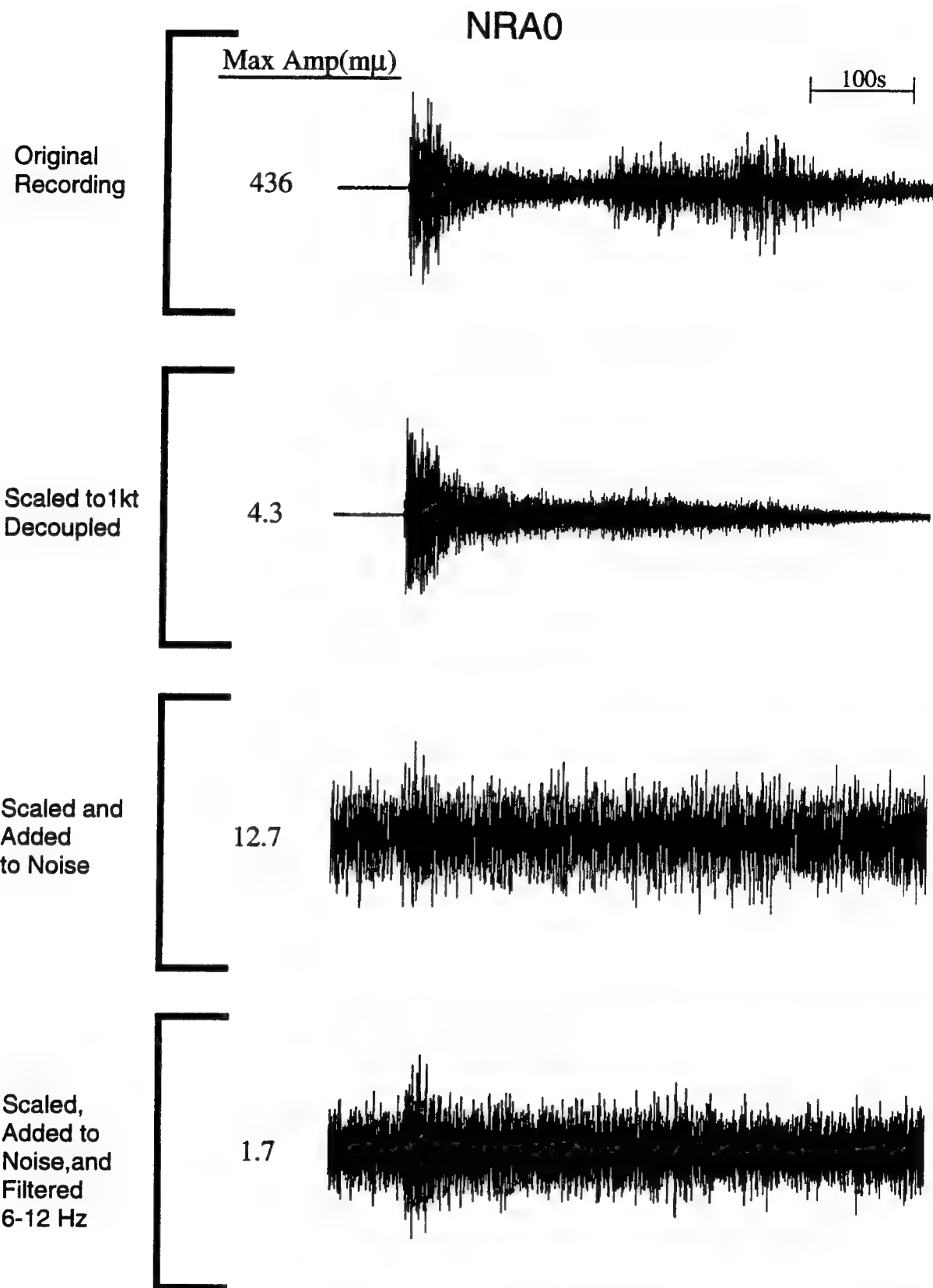


Figure 5. Examples of application of source-scaling process to PNE explosion at NORESS.

complex regional P, regional S, and separate Lg. After scaling, the broadband time history is reduced in maximum amplitude by a factor of about 100. As was noted in the previous example, the P signal is relatively more prominent; and the regional S and particularly Lg signals are significantly reduced. This again can probably be explained by relatively greater high-frequency content in the P signal and the shift toward high frequencies caused by the scaling operation. In the third trace we see the scaled record at NRAO added to the 4/23/92 noise. The scaled signal is again much smaller than (about a factor of three) the maximum broadband noise level, so the 1-kt explosion signal is not apparent relative to the background noise. We again applied bandpass filtering to the records covering a range of frequency bands. Again there was no indication of regional signals in the low-frequency passbands, but high-frequency bandpass filters again bring out the P signal. However, in this case later regional S and Lg signals remain below the noise in all passbands.

Figures 6 and 7 illustrate the effects of the scaling process in the spectral domain. The plots compare Fourier spectra for 50-second segments of the regional P and S signals at ARA0 for the 10/24/90 NZ explosion before and after application of the scaling. We also computed the Fourier spectrum for a noise segment of similar length. Comparing the original and scaled regional P-wave spectra, we see a large difference in spectral level (averaging about a factor of 1000) over the frequency interval from 0.5 to above 2 Hz. Between 2 Hz and about 8 Hz, the difference in the spectral level drops off rather rapidly from a factor of about 1000 to a factor of only about 40 and then remains at a factor of 20-30 out to near 20 Hz. Comparing the signal spectra to the noise spectrum, the original explosion P signal is well above noise over the entire frequency band from 0.5 to 20 Hz. However, the P-wave spectrum scaled to 1-kt decoupled falls below the background noise out to beyond 2 Hz. The scaled P spectrum gradually rises above the noise over the interval from 2 Hz to 8 Hz with S/N averaging about five. Above 8 Hz the S/N continues to increase with frequency averaging about ten. The behavior for the regional S spectra in Figure 7 is similar. Differences in the regional S spectra between the original and scaled records are the same as



Figure 6. Comparison of regional P-wave Fourier spectra determined from ARA0 record of 10/24/90 NZ explosion before and after scaling to 1kt decoupled relative to spectrum of background noise.

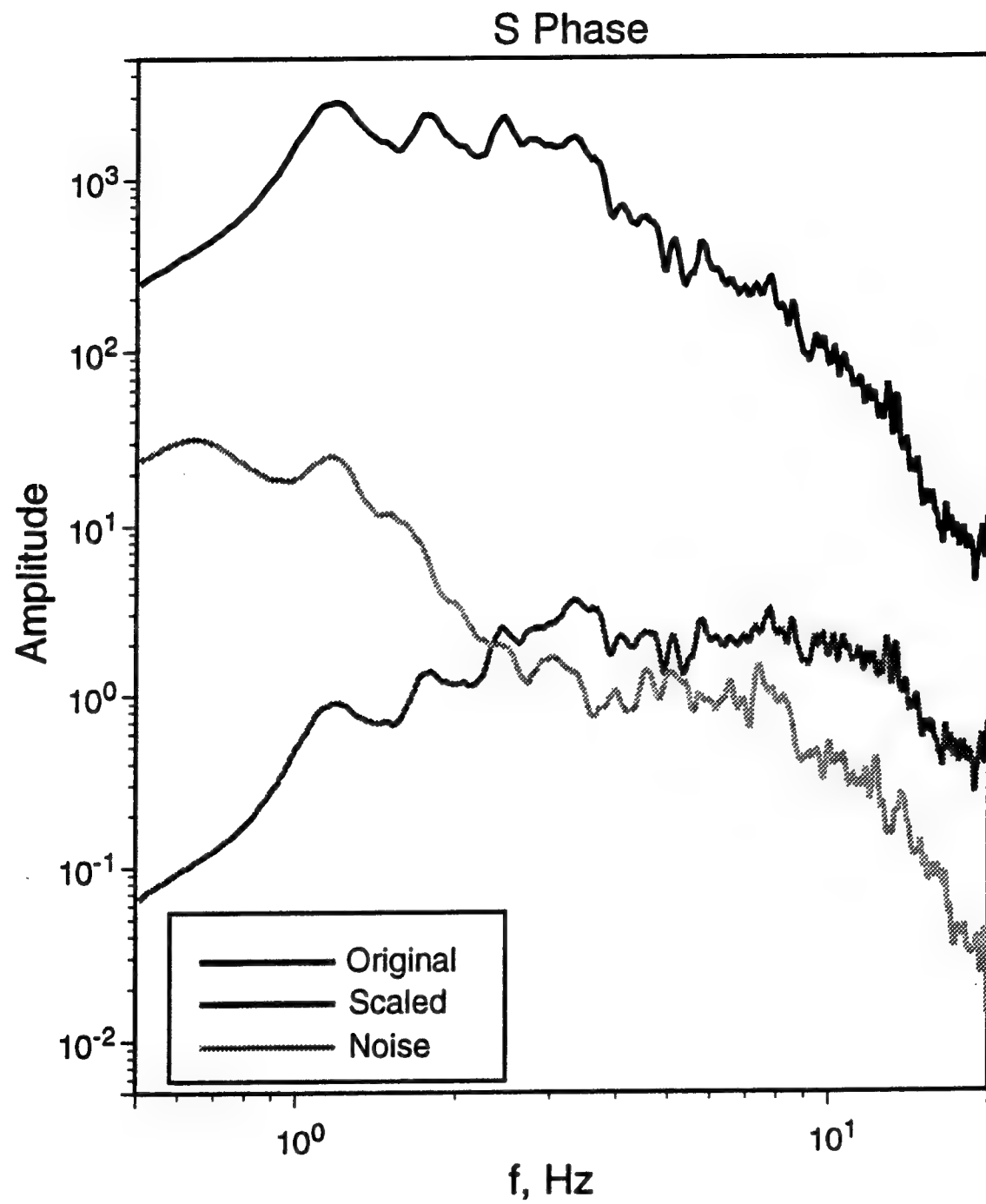


Figure 7. Comparison of regional S-wave Fourier spectra determined from ARA0 record of 10/24/90 NZ explosion before and after scaling to 1kt decoupled relative to spectrum of background noise.

those seen for P since the same scaling factor has been applied to each. The regional S spectrum for the scaled record rises above the noise between 2 and 3 Hz. However, the S/N is generally lower than for the regional P, averaging only about 2 - 3 over the interval from 2 Hz to 8 Hz. Above 8 Hz the S/N continues to increase for the scaled S averaging about five. Thus, the useful frequency band for such small events at far-regional stations is restricted to relatively high frequencies; and, at larger distances or with higher background noise, the frequency band useful for analysis of regional signals from small events is likely to be even more restricted.

Figure 8 presents extended waveform segments for a larger sample of ARCESS array channels obtained from the same scaling process described above in Figure 4. These were selected from the complete array records produced from the scaling applied to each of the explosions for the two alternative noise segments. On the broadband channels in Figure 8, the S/N level is at or below one; so there is little evidence of regional signals on these traces. As noted above, the broadband channels in this regional distance range and beyond do not seem to be particularly useful for detecting signals from such small, decoupled nuclear explosions. However, Figure 9 shows the same traces with the 6 - 12 Hz bandpass filter applied. Here the regional P and S or Lg signals stand out above the background noise with S/N between 3:1 and 5:1. The results again indicate that higher frequencies are likely to be more useful for detecting regional signals and for identifying source types for small regional events.

4.2 Comparison to Prior Studies

Detection thresholds for the ARPA regional arrays in Fennoscandia have been previously analyzed by Ringdal and Kvaerna (1989), Kvaerna and Ringdal (1990, 1991), Fyen (1990), and Kvaerna (1992). Ringdal and Kvaerna (1989) used an array-processing technique, termed generalized beamforming, to direct the three Fennoscandia arrays at locations throughout the region and assess capability. They showed that noise level measurements obtained from continuous monitoring (Continuous Seismic Threshold

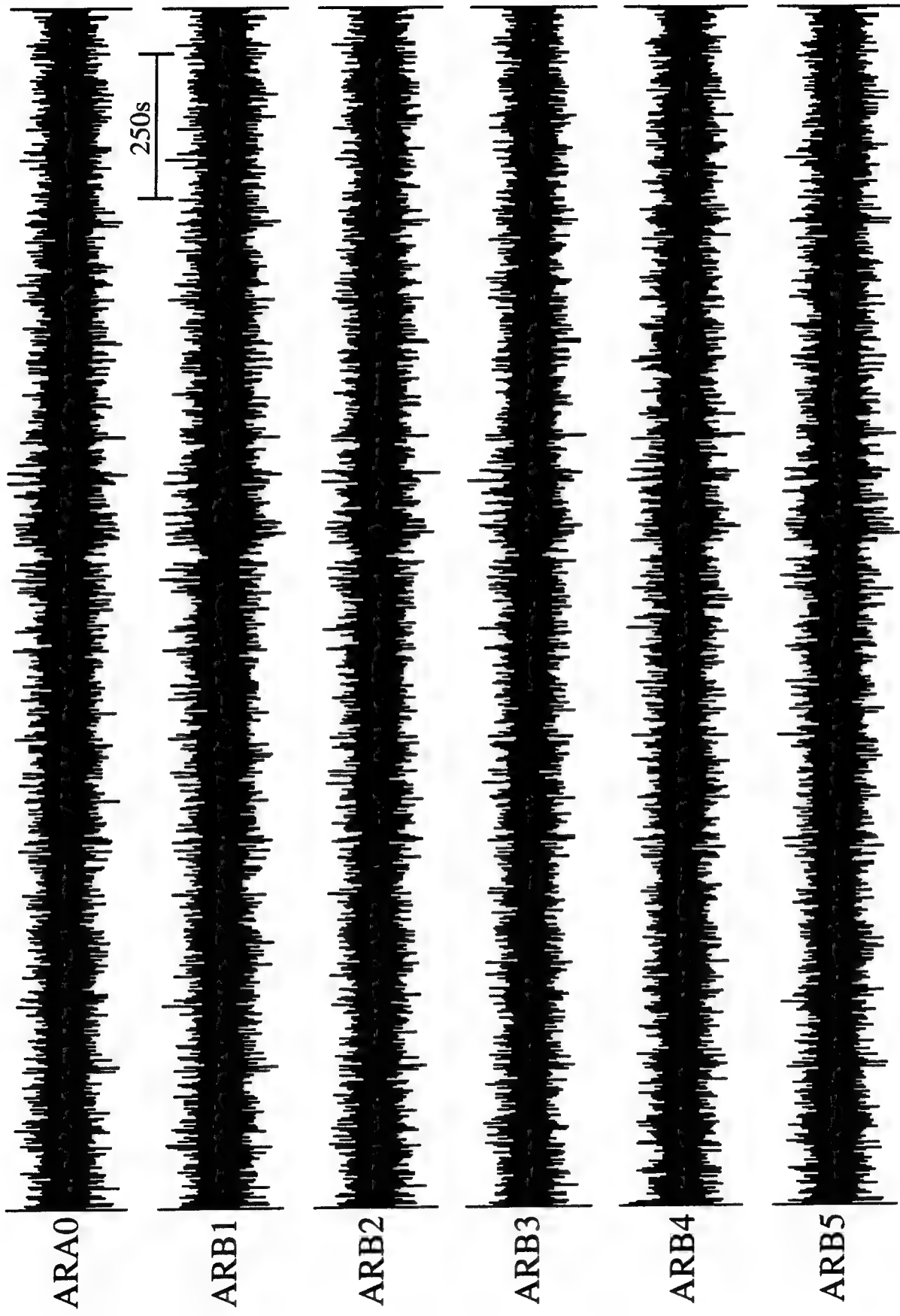


Figure 8. Extended broadband waveform segments for selected ARCESS elements simulating a 1kton decoupled nuclear explosion from NZ embedded in typical background noise.

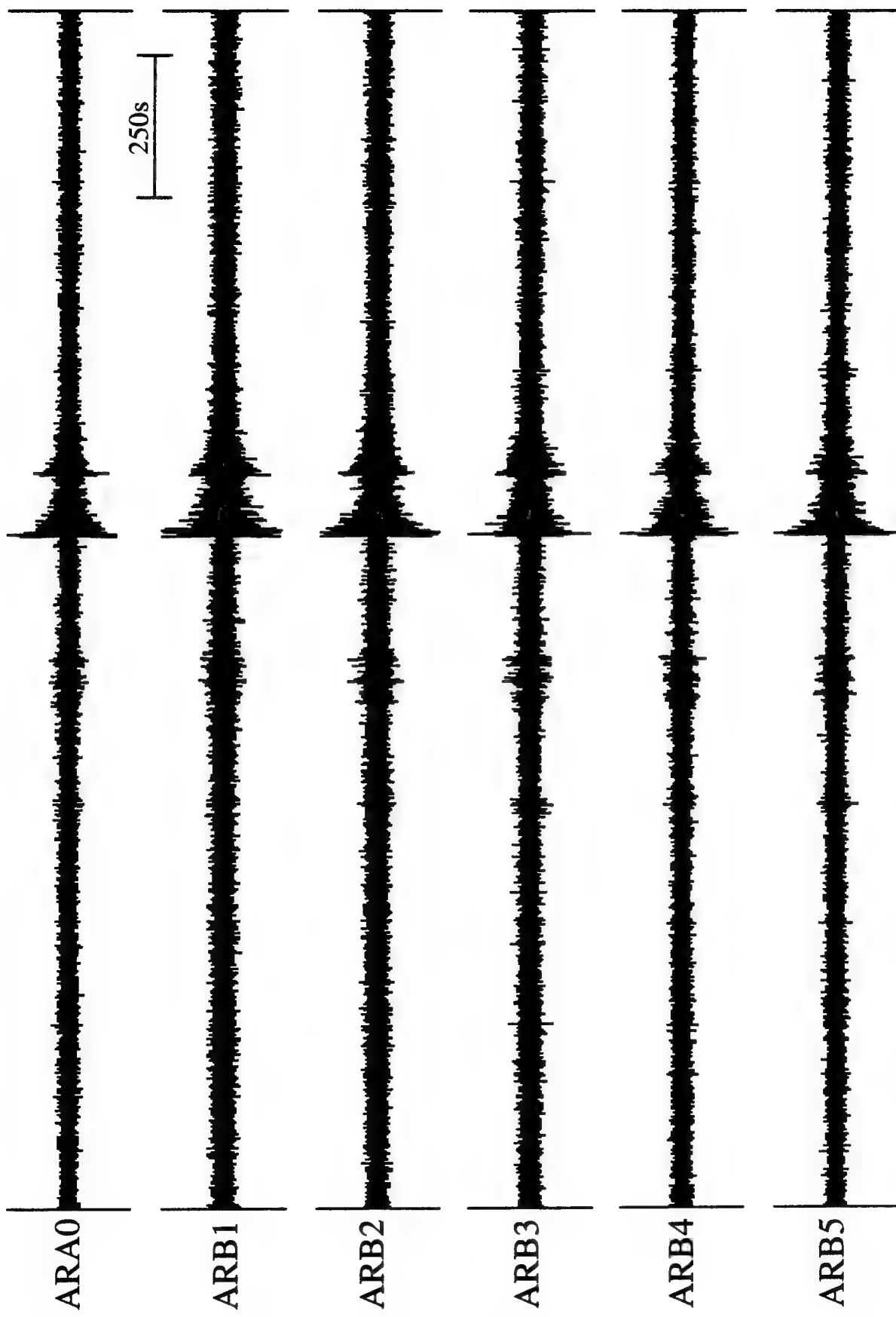


Figure 9. Bandpass filtered (6-12 Hz) waveform segments for the same channels for the simulation of a 1kt decoupled nuclear explosion from NZ in typical background noise.

Monitoring) could be used to obtain individual array and combined array estimates of the detection thresholds for regional phase signals from various source areas. Kvaerna and Ringdal (1990) applied this methodology to the area of the northern Novaya Zemlya test site. They found for a one-week period that Novaya Zemlya could generally be monitored to a magnitude level approaching 2.5 mb using the data from the ARCESS, NORESS, and FINESA regional arrays. Times when the threshold rose above this level corresponded to times when the records at the arrays were enhanced due to observed signals from teleseismic or regional events.

Kvaerna (1992) applied Continuous Seismic Threshold Monitoring to a longer time period covering the month of February, 1992. He found that the magnitude detection threshold for Novaya Zemlya was lower than 2.5 mb more than 99 percent of the time. He also found that the ARCESS array, which is nearest to NZ ($R \approx 1100$ km), was critical to maintaining the low monitoring threshold for that source area. On average, the ARCESS array detection threshold was at least 0.3 magnitude units lower than that of NORESS and about 0.4 magnitude units lower than that of FINESA. The comparison for ARCESS and NORESS is illustrated in Figure 10 which shows the magnitude levels corresponding to background noise levels (excluding brief exceedences). One interesting aspect of the background noise illustrated in the figure is that the NORESS noise level remains fairly stable while the ARCESS noise shows some rather strong fluctuations. The variations in the threshold at ARCESS are more than 0.5 magnitude units, from about 2.0 mb during quiet noise conditions to about 2.6 mb during high noise. These high-noise conditions at ARCESS are believed to correlate with high winds and severe weather (cf. Kvaerna, 1992). In comparison, the thresholds at NORESS vary between about 2.5 and 2.7 mb over the month. Fyen (1990) found that for NORESS the diurnal variations in noise were small for frequencies below about 2 Hz, but somewhat higher differences (viz. 0.2 - 0.3 mb units) were found between daytime and nighttime noise levels at higher frequencies. The FINESA thresholds, which are not shown, appear to depend mainly on cultural noise with indications of both diurnal and weekly variations. The variability in

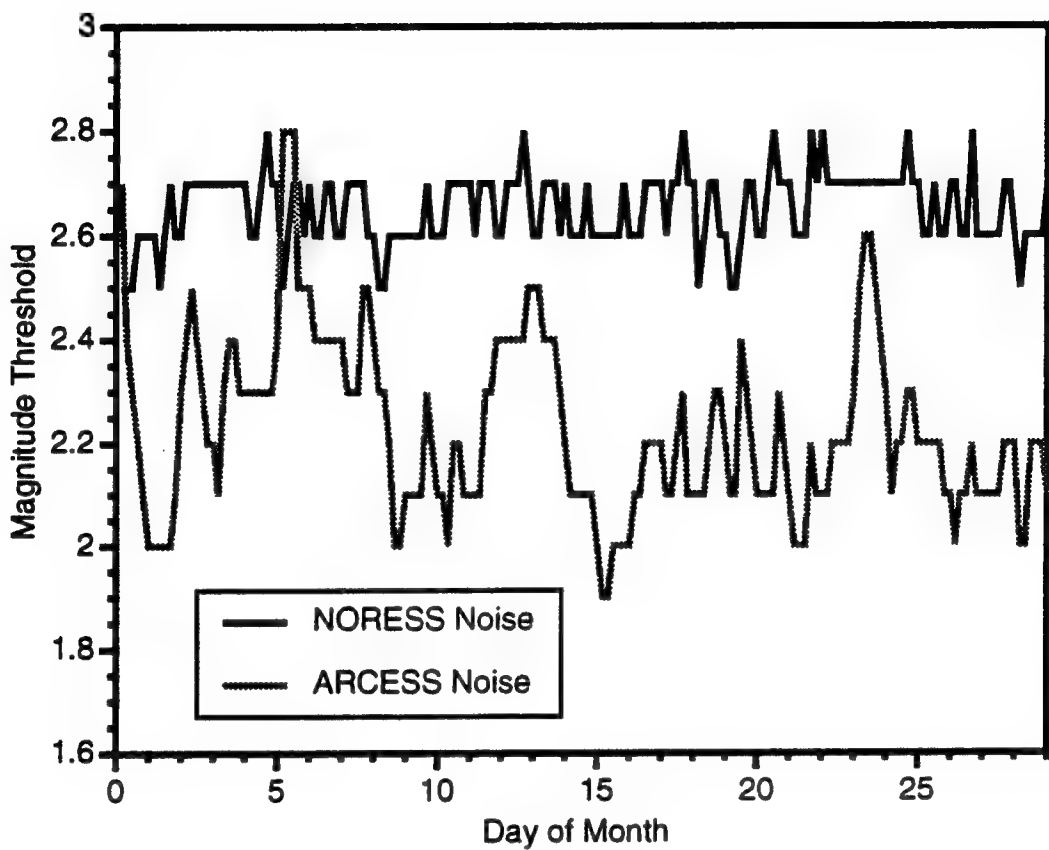


Figure 10. Variations in monitoring thresholds from Novaya Zemlya (excluding time intervals of observed events) for the NORESS and ARCESS regional arrays during the month of February, 1992 (adapted from Kvaerna, 1992).

noise levels and corresponding detection thresholds at the critical ARCESS array over the single month of observations suggest that additional work may be useful to establish more long-term characteristics of regional monitoring thresholds.

Kvaerna and Ringdal (1991) also performed scaling analysis on the large Novaya Zemlya nuclear explosion test of October 24, 1990. However, unlike our analyses (presented above), which accounted for frequency dependence related to explosion source size, the Kvaerna and Ringdal analysis was based on simple magnitude scaling. Thus, in scaling down from the original explosion magnitude of 5.6 mb to 2.6 mb, the trace amplitudes were simply divided by a factor of 1000 and added back into background noise. Kvaerna and Ringdal found that far-regional P and S signals in a passband 3 - 5 Hz could be seen easily on P and S array beams at ARCESS for both nighttime (low) and daytime (high) noise conditions. P signals were also visible in the passband 2 - 4 Hz on P array beams at FINESA for both nighttime and daytime noise. Although P was also visible at NORESS for both nighttime and daytime noise, the S/N level was approaching one for both cases. The results of the scaling analysis by Kvaerna and Ringdal would appear to be somewhat more optimistic than our results with regard to detectability of regional signals from small events. In spite of the fact that our scaling procedure should enhance the higher-frequency content of signals and make them more easily detectable, we are not seeing the high-frequency regional signals at the more-distant stations as well as Kvaerna and Ringdal. Besides the scaling procedures, the main differences between the Kvaerna/Ringdal study and ours, would appear to be their use of beam-forming techniques in processing the array signals and the different record samples used as background noise segments. Additional study is required to determine whether these procedural differences can account for the observations.

4.3 Comparison to the December 31, 1992 NZ Event

As a final test of these procedures and their relevance to discrimination, we have compared the results obtained from scaling the NZ nuclear explosion with the observations from the unknown

seismic event which occurred at NZ (73.5 N, 55.5 E) on December 31, 1992 (cf. Ryall, 1993). This unknown event was estimated by NORSTAR to have had a magnitude of about 2.5 and should be quite comparable to the 1-kt fully-decoupled nuclear explosion ($m_b = 2.6$) which was simulated above. We focus here on a comparison of the band-pass filter analyses which we performed on the center-element, vertical-component records at the ARCESS array, which recorded the best signals from the events. Figures 11 and 12 show the results of the band-pass filter analyses on respectively the 12/31/92 unknown event and the 10/24/90 NZ explosion scaled to 1-kt decoupled and added back into background noise. We first note that there is no indication of any signals on the records for filter passbands below 3 Hz, as S/N in these frequency bands is less than one. Pn and Sn signals are apparent for all the higher frequency passbands for both events, but there is little indication of Lg for either. The Sn signal and its coda appear to be better developed for the 12/31/92 event. For frequency bands between about 3 and 16 Hz, we see that S/P ratios for the 12/31/92 event are greater than 1.0. In contrast, over the same bands the maximum S/P ratios for the 10/24/90 NZ explosion scaled to 1-kt decoupled are only about 0.5. Although it cannot be seen in the figure since the traces are individually normalized, the maximum amplitudes of the P signals in the frequency band above about 3 Hz are a factor of two or more larger for the scaled explosion than for the unknown event. We plan to perform similar comparisons for other events as this research progresses.

We would interpret this preliminary result to indicate that the 12/31/92 unknown event at NZ has far-regional signal characteristics at ARCESS different from what would be expected from an underground nuclear explosion of comparable magnitude. The behavior in the S/P ratios at regional distances is similar to that seen in Fennoscandia and other parts of the world where the ratios for earthquakes tend to maintain a level at or above 1.0 over a broad band out to high frequencies while similar ratios for explosions tend to drop off rapidly to well below 1.0 at high frequencies. This behavior would be consistent with interpretation of the 12/31/92 event as an earthquake.

ARCESS

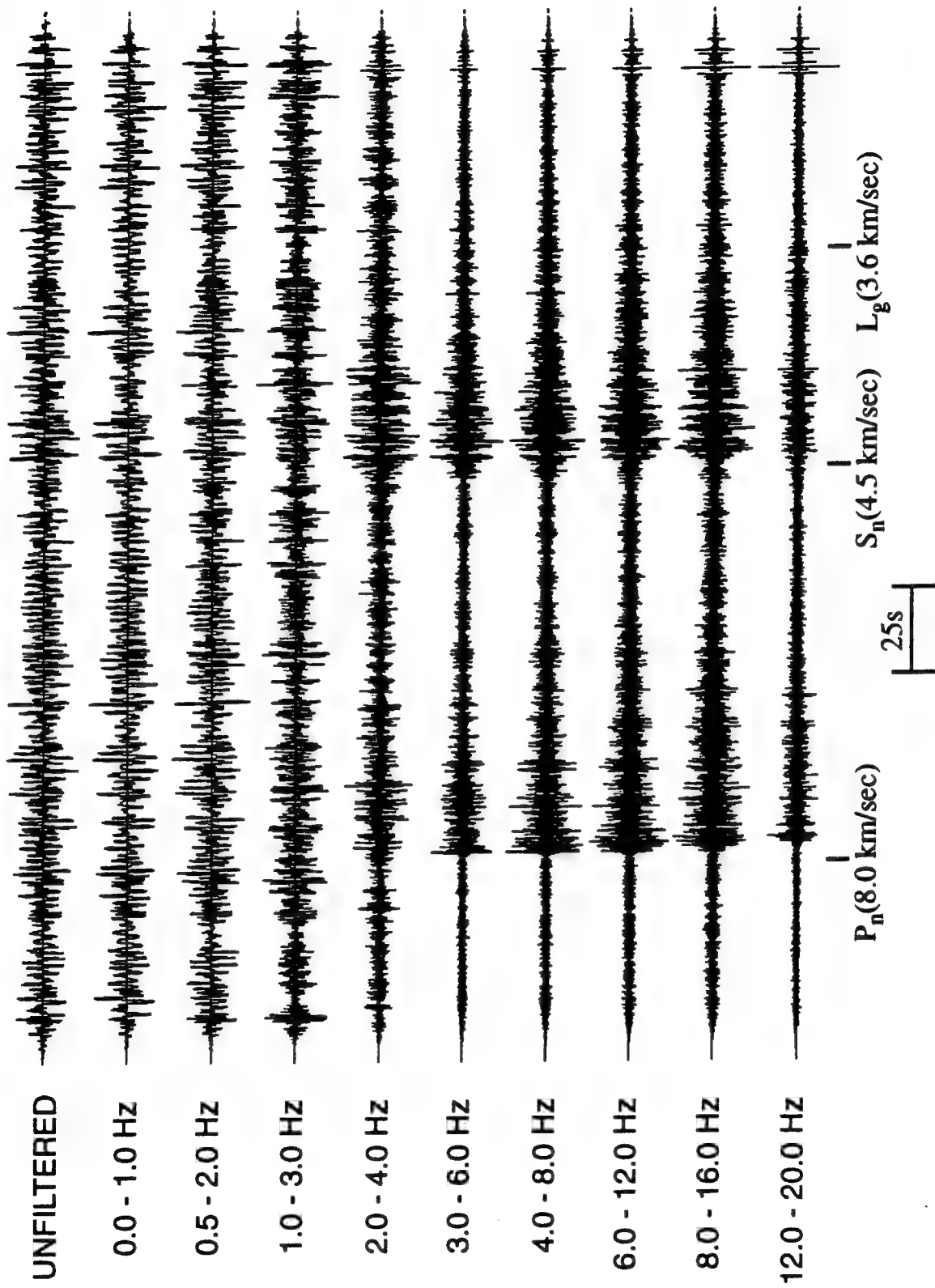


Figure 11. Application of band-pass filter analysis to vertical-component ARA0 recording of the 12/31/92 unknown event at Novaya Zemlya.

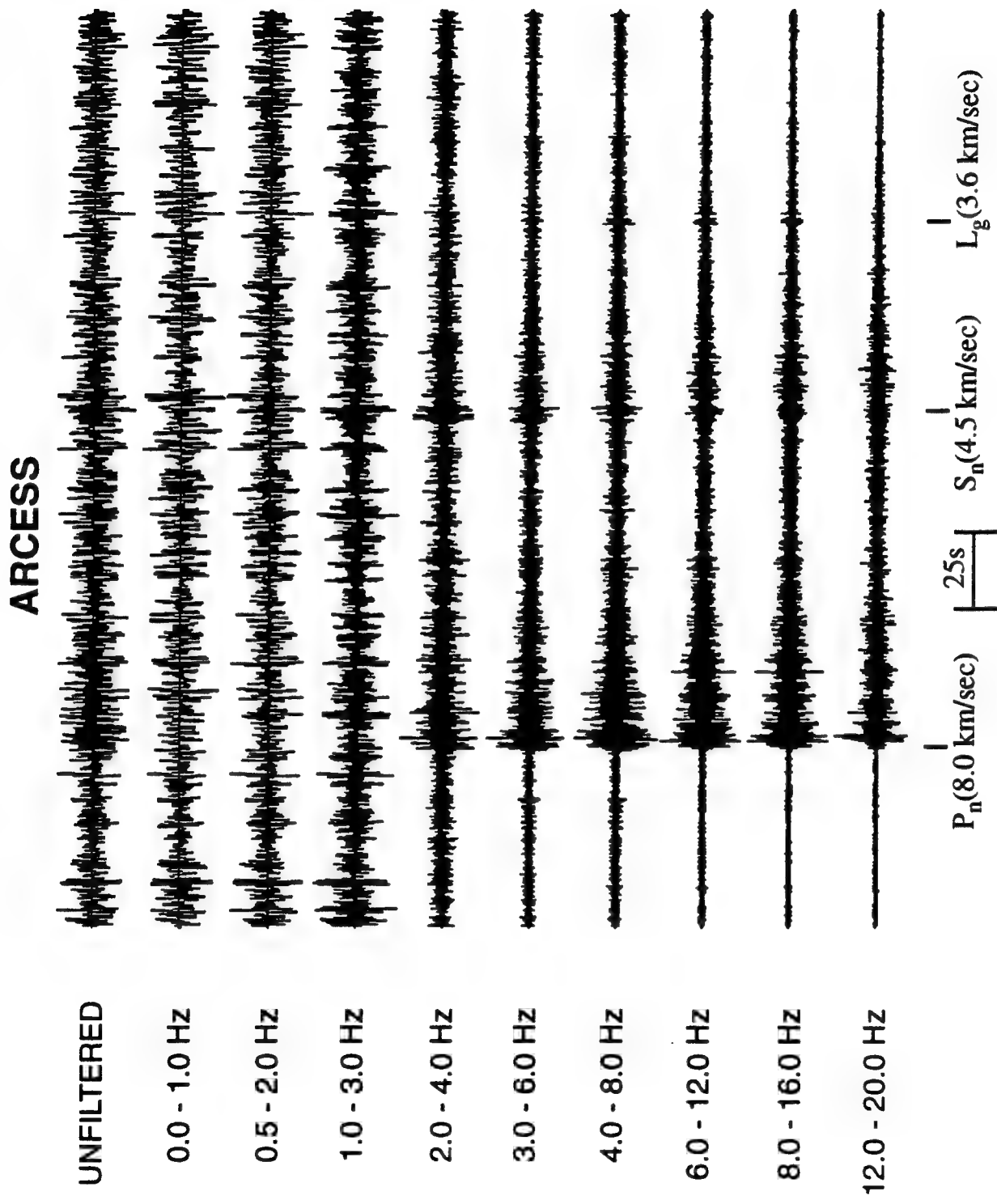


Figure 12. Application of band-pass filter analysis to vertical-component ARA0 recording of the 10/24/90 NZ explosion scaled down to 1kt fully decoupled.

5. Summary and Conclusions

In this research program we have used source-scaling theory to investigate potential seismic identification problems associated with small or decoupled nuclear explosions under a CTBT or near a low monitoring threshold. In particular, Mueller-Murphy scaling has been used to modify observed seismograms recorded at the ARPA regional array stations in Fennoscandia. The seismic signals from large, well-recorded nuclear explosion tests from the nuclear test site at Novaya Zemlya and a large PNE test north of Arkhangel'sk have been scaled down to simulate the signals from a 1-kt fully decoupled underground explosion. These scaled seismic signals, embedded in records representative of the background noise at the regional stations, were then used to assess the limitations on detection and identification capabilities of regional signal analysis methods at the lower thresholds. We have reviewed time-domain amplitude and spectral behavior of the scaled signals relative to representative samples of background noise to determine signal-to-noise levels and to identify limits on the frequency bands of regional signals which are likely to be useful for discrimination of small events.

As part of this effort, a digital data tape was also provided to the Center for Seismic Studies for use in testing capabilities of the monitoring system for small events. The data tape included full-array data obtained by applying the source scaling procedures to three different events and, then, reintroducing the scaled signals into two different segments of representative background noise. We believe that these data provide reasonable simulations of the seismic signals at the Fennoscandian regional arrays which would be expected from far-regional 1-kt fully decoupled nuclear explosions. These data should enable a valid test of detection, location, and seismic identification capabilities of these regional arrays for monitoring small or decoupled nuclear explosion tests under a CTBT.

Our preliminary observations based on these simulations are that the seismic signals from nuclear explosions at a threshold level near 1-kt fully decoupled could be difficult to discern on broadband records at far-regional stations. The useful signals from such small or

decoupled explosions may be constrained to rather limited high-frequency bands. At farther regional distances attenuation is also likely to play a role in limiting the high-frequency content of regional signals. These kinds of limitations would tend to restrict the available frequency band of regional phases for use in detection, location, and discrimination of seismic events. Some regional discrimination techniques may be impaired more than others by such frequency limitations (e.g. techniques which compare regional signal properties over a broadband may not be applicable). Although array processing techniques are likely to provide some improvement in overall signal detectability, we have not yet specifically considered how such procedures affect these conclusions. Further work is needed to refine the character of the frequency-band limitations and their influences on discriminant measures and regional detection and location capabilities for various regions of interest. We also plan to review additional noise samples to see how noise conditions at different times of the day and year might affect our conclusions regarding the detectability of the regional signals from small, decoupled explosions.

Finally, with regard to specific discrimination results, comparison of band-pass filter results from the 12/31/92 unknown event at Novaya Zemlya and from the simulation of a 1-kt fully decoupled explosion at the common ARCESS recording station indicates a larger S/P ratio for the unknown event at frequencies above about 3 Hz. These differences appear to be associated with more high-frequency P-wave energy in the explosion source. Based on these comparisons the 12/31/92 unknown event at NZ is considered to be more typical of an earthquake.

6. References

- Bache, T. C. (1982). "Estimating the Yield of Underground Nuclear Explosions," *Bull. Seism. Soc. Am.* 72, pp. S131 - S168.
- Fyen, J. (1990). "Diurnal and Seasonal Variations in the Microseismic Noise Level Observed at the NORESS Array," *Phys. Earth Planet. Inter.* 63, pp. 252 - 268.
- Kvaerna, T. (1992). "Continuous Seismic Threshold Monitoring of the Northern Novaya Zemlya Test Site: Long-Term Operational Characteristics," Report PL-TR-92-2118, Phillips Laboratory, Hanscom Air Force Base, MA, ADA252890.
- Kvaerna, T., and F. Ringdal (1990). "Continuous Threshold Monitoring of the Novaya Zemlya Test Site," in *Semiannual Technical Summary, 1 Apr - 30 Sep 1990*, NORSAR Sci. Rep. 1-90/91, NORSAR, Kjeller, Norway.
- Kvaerna, T., and F. Ringdal (1991). "Threshold Monitoring of Novaya Zemlya: A Scaling Experiment," in *Semiannual Technical Summary, 1 Oct 1990 - 31 Mar 1991*, NORSAR Sci. Rep. 1-90/91, NORSAR, Kjeller, Norway.
- Mueller, R. A., and J. R. Murphy (1971). "Seismic Characteristics of Underground Nuclear Detonations. Part I. Seismic Spectrum Scaling," *Bull. Seism. Soc. Am.* 61, pp. 1675 - 1692.
- Murphy, J. R. (1977). "Seismic Source Functions and Magnitude Determinations for Underground Nuclear Detonations," *Bull. Seism. Soc. Am.* 67, pp. 135 - 158.
- Office of Technology Assessment (1988). *Seismic Verification of Nuclear Testing Treaties*, U. S. Congress OTA Report No. OTA-ISC-361.
- Ringdal, F., and T. Kvaerna (1989). "A Multi-Channel Processing Approach to Real-Time Network Detection, Phase Association, and Threshold Monitoring," *Bull. Seism. Soc. Am.* 79, pp. 1927 - 1940.
- Ringdal, F., P. D. Marshall, and R. W. Alewine (1992). "Seismic Yield Determination of Soviet Underground Nuclear Explosions at the Shagan River Test Site," *Geophys. J. Int.* 109, pp. 65 - 77.

- Rodean, H. C. (1981). "Inelastic Processes in Seismic Wave Generation by Underground Explosions," in *Identification of Seismic Sources -- Earthquake or Underground Explosion*, Proc. of NATO ASI, Reidel Publishing Co., Dordrecht, Holland, pp. 97 - 189.
- Ryall, A. S. (1993). The Novaya Zemlya Event of 31 December 1992 and Seismic Identification Issues, Executive Summary, Published in Conjunction with the 15th Annual Seismic Research Symposium, 8 - 10 September 1993, Vail, Colorado.
- Vergino, E. S. (1989a). "Soviet Test Yields," *EOS* 70, pp. 1511 - 1524.
- Vergino, E. S. (1989b). "Soviet Test Yields, Corrections and Additions," *EOS* 70, p. 1569.
- von Seggern, D. H., and R. R. Blandford (1972). "Source Time Functions and Spectra for Underground Nuclear Explosions," *Geophys. J.* 31, pp. 83 - 97.

Prof. Thomas Ahrens
Seismological Lab, 252-21
Division of Geological & Planetary Sciences
California Institute of Technology
Pasadena, CA 91125

Prof. Keiiti Aki
Center for Earth Sciences
University of Southern California
University Park
Los Angeles, CA 90089-0741

Prof. Shelton Alexander
Geosciences Department
403 Deike Building
The Pennsylvania State University
University Park, PA 16802

Dr. Thomas C. Bache, Jr.
Science Applications Int'l Corp.
10260 Campus Point Drive
San Diego, CA 92121 (2 copies)

Prof. Muawia Barazangi
Cornell University
Institute for the Study of the Continent
3126 SNEE Hall
Ithaca, NY 14853

Dr. Douglas R. Baumgardt
ENSCO, Inc
5400 Port Royal Road
Springfield, VA 22151-2388

Dr. T.J. Bennett
S-CUBED
A Division of Maxwell Laboratories
11800 Sunrise Valley Drive, Suite 1212
Reston, VA 22091

Dr. Robert Blandford
AFTAC/TT, Center for Seismic Studies
1300 North 17th Street
Suite 1450
Arlington, VA 22209-2308

Dr. Steven Bratt
ARPA/NMRO
3701 North Fairfax Drive
Arlington, VA 22203-1714

Dale Breding
U.S. Department of Energy
Recipient, IS-20, GA-033
Office of Arms Control
Washington, DC 20585

Dr. Jerry Carter
Center for Seismic Studies
1300 North 17th Street
Suite 1450
Arlington, VA 22209-2308

Mr Robert Cockerham
Arms Control & Disarmament Agency
320 21st Street North West
Room 5741
Washington, DC 20451,

Dr. Zoltan Der
ENSCO, Inc.
5400 Port Royal Road
Springfield, VA 22151-2388

Dr. Stanley K. Dickinson
AFOSR/NM
110 Duncan Avenue
Suite B115
Bolling AFB, DC

Dr Petr Firbas
Institute of Physics of the Earth
Masaryk University Brno
Jecna 29a
612 46 Brno, Czech Republic

Dr. Mark D. Fisk
Mission Research Corporation
735 State Street
P.O. Drawer 719
Santa Barbara, CA 93102

Dr. Cliff Frolich
Institute of Geophysics
8701 North Mopac
Austin, TX 78759

Dr. Holly Given
IGPP, A-025
Scripps Institute of Oceanography
University of California, San Diego
La Jolla, CA 92093

Dr. Jeffrey W. Given
SAIC
10260 Campus Point Drive
San Diego, CA 92121

Dr. Dale Glover
Defense Intelligence Agency
ATTN: ODT-1B
Washington, DC 20301

Dan N. Hagedon
Pacific Northwest Laboratories
Battelle Boulevard
Richland, WA 99352

Robert C. Kemerait
ENSCO, Inc.
445 Pineda Court
Melbourne, FL 32940

Dr. James Hannon
Lawrence Livermore National Laboratory
P.O. Box 808, L-205
Livermore, CA 94550

U.S. Dept of Energy
Max Koontz, NN-20, GA-033
Office of Research and Develop.
1000 Independence Avenue
Washington, DC 20585

Dr. Roger Hansen
University of Colorado, JSPC
Campus Box 583
Boulder, CO 80309

Dr. Richard LaCoss
MIT Lincoln Laboratory, M-200B
P.O. Box 73
Lexington, MA 02173-0073

Prof. David G. Harkrider
Division of Geological & Planetary Sciences
California Institute of Technology
Pasadena, CA 91125

Prof. Charles A. Langston
Geosciences Department
403 Deike Building
The Pennsylvania State University
University Park, PA 16802

Prof. Danny Harvey
University of Colorado, JSPC
Campus Box 583
Boulder, CO 80309

Jim Lawson, Chief Geophysicist
Oklahoma Geological Survey
Oklahoma Geophysical Observatory
P.O. Box 8
Leonard, OK 74043-0008

Prof. Donald V. Helmberger
Division of Geological & Planetary Sciences
California Institute of Technology
Pasadena, CA 91125

Prof. Thorne Lay
Institute of Tectonics
Earth Science Board
University of California, Santa Cruz
Santa Cruz, CA 95064

Prof. Eugene Herrin
Geophysical Laboratory
Southern Methodist University
Dallas, TX 75275

Dr. William Leith
U.S. Geological Survey
Mail Stop 928
Reston, VA 22092

Prof. Robert B. Herrmann
Department of Earth & Atmospheric Sciences
St. Louis University
St. Louis, MO 63156

Mr. James F. Lewkowicz
Phillips Laboratory/GPE
29 Randolph Road
Hanscom AFB, MA 01731-3010(2 copies)

Prof. Lane R. Johnson
Seismographic Station
University of California
Berkeley, CA 94720

Dr. Gary McCartor
Department of Physics
Southern Methodist University
Dallas, TX 75275

Prof. Thomas H. Jordan
Department of Earth, Atmospheric &
Planetary Sciences
Massachusetts Institute of Technology
Cambridge, MA 02139

Prof. Thomas V. McEvilly
Seismographic Station
University of California
Berkeley, CA 94720

Dr. Keith L. McLaughlin
S-CUBED
A Division of Maxwell Laboratory
P.O. Box 1620
La Jolla, CA 92038-1620

Prof. Bernard Minster
IGPP, A-025
Scripps Institute of Oceanography
University of California, San Diego
La Jolla, CA 92093

Prof. Brian J. Mitchell
Department of Earth & Atmospheric Sciences
St. Louis University
St. Louis, MO 63156

Mr. Jack Murphy
S-CUBED
A Division of Maxwell Laboratory
11800 Sunrise Valley Drive, Suite 1212
Reston, VA 22091 (2 Copies)

Dr. Keith K. Nakanishi
Lawrence Livermore National Laboratory
L-025
P.O. Box 808
Livermore, CA 94550

Prof. John A. Orcutt
IGPP, A-025
Scripps Institute of Oceanography
University of California, San Diego
La Jolla, CA 92093

Dr. Howard Patton
Lawrence Livermore National Laboratory
L-025
P.O. Box 808
Livermore, CA 94550

Dr. Frank Pilotte
HQ AFTAC/TT
1030 South Highway A1A
Patrick AFB, FL 32925-3002

Dr. Jay J. Pulli
Radix Systems, Inc.
201 Perry Parkway
Gaithersburg, MD 20877

Prof. Paul G. Richards
Lamont-Doherty Earth Observatory
of Columbia University
Palisades, NY 10964

Mr. Wilmer Rivers
Multimax Inc.
1441 McCormick Drive
Landover, MD 20785

Dr. Alan S. Ryall, Jr.
Lawrence Livermore National Laboratory
L-025
P.O. Box 808
Livermore, CA 94550

Dr. Chandan K. Saikia
Woodward Clyde- Consultants
566 El Dorado Street
Pasadena, CA 91101

Mr. Dogan Seber
Cornell University
Inst. for the Study of the Continent
3130 SNEE Hall
Ithaca, NY 14853-1504

Secretary of the Air Force
(SAFRD)
Washington, DC 20330

Office of the Secretary of Defense
DDR&E
Washington, DC 20330

Thomas J. Sereno, Jr.
Science Application Int'l Corp.
10260 Campus Point Drive
San Diego, CA 92121

Dr. Michael Shore
Defense Nuclear Agency/SPSS
6801 Telegraph Road
Alexandria, VA 22310

Prof. David G. Simpson
IRIS, Inc.
1616 North Fort Myer Drive
Suite 1050
Arlington, VA 22209

Dr. Jeffrey Stevens
S-CUBED
A Division of Maxwell Laboratory
P.O. Box 1620
La Jolla, CA 92038-1620

Prof. Brian Stump
Los Alamos National Laboratory
EES-3
Mail Stop C-335
Los Alamos, NM 87545

TACTEC
Battelle Memorial Institute
505 King Avenue
Columbus, OH 43201 (Final Report)

Prof. Tuncay Taymaz
Istanbul Technical University
Dept. of Geophysical Engineering
Mining Faculty
Maslak-80626, Istanbul Turkey

Phillips Laboratory
ATTN: GPE
29 Randolph Road
Hanscom AFB, MA 01731-3010

Prof. M. Nafi Toksoz
Earth Resources Lab
Massachusetts Institute of Technology
42 Carleton Street
Cambridge, MA 02142

Phillips Laboratory
ATTN: TSML
5 Wright Street
Hanscom AFB, MA 01731-3004

Dr. Larry Turnbull
CIA-OSWR/NED
Washington, DC 20505

Phillips Laboratory
ATTN: PL/SUL
3550 Aberdeen Ave SE
Kirtland, NM 87117-5776 (2 copies)

Dr. Karl Veith
EG&G
5211 Auth Road
Suite 240
Suitland, MD 20746

Dr. Michel Campillo
Observatoire de Grenoble
I.R.I.G.M.-B.P. 53
38041 Grenoble, FRANCE

Prof. Terry C. Wallace
Department of Geosciences
Building #77
University of Arizona
Tuscon, AZ 85721

Dr. Kin Yip Chun
Geophysics Division
Physics Department
University of Toronto
Ontario, CANADA

Dr. William Wortman
Mission Research Corporation
8560 Cinderbed Road
Suite 700
Newington, VA 22122

Prof. Hans-Peter Harjes
Institute for Geophysic
Ruhr University/Bochum
P.O. Box 102148
4630 Bochum 1, GERMANY

ARPA, OASB/Library
3701 North Fairfax Drive
Arlington, VA 22203-1714

Prof. Eystein Husebye
NTNF/NORSAR
P.O. Box 51
N-2007 Kjeller, NORWAY

HQ DNA
ATTN: Technical Library
Washington, DC 20305

David Jepsen
Acting Head, Nuclear Monitoring Section
Bureau of Mineral Resources
Geology and Geophysics
G.P.O. Box 378, Canberra, AUSTRALIA

Defense Technical Information Center
Cameron Station
Alexandria, VA 22314 (2 Copies)

Ms. Eva Johannsson
Senior Research Officer
FOA
S-172 90 Sundbyberg, SWEDEN

**Dr. Peter Marshall
Procurement Executive
Ministry of Defense
Blacknest, Brimpton
Reading FG7-FRS, UNITED KINGDOM**

**Dr. Bernard Massinon, Dr. Pierre Mechler
Societe Radiomana
27 rue Claude Bernard
75005 Paris, FRANCE (2 Copies)**

**Dr. Svein Mykkeltveit
NTNT/NORSAR
P.O. Box 51
N-2007 Kjeller, NORWAY (3 Copies)**

**Dr. Jorg Schlittenhardt
Federal Institute for Geosciences & Nat'l Res.
Postfach 510153
D-30631 Hannover , GERMANY**

**Dr. Johannes Schweitzer
Institute of Geophysics
Ruhr University/Bochum
P.O. Box 1102148
4360 Bochum 1, GERMANY**

**Trust & Verify
VERTIC
Carrara House
20 Embankment Place
London WC2N 6NN, ENGLAND**